Research in Astron. Astrophys. **2013** Vol. **13** No. **12**, 1455–1462
http://www.raa-journal.org *http://www.iop.org/journals/raa*

***R**esearch in*
***A**stronomy and*
***A**strophysics*

Mass flow in a circumbinary disk with a gap around supermassive binary black holes *

Ning-Yu Tang and Ye-Fei Yuan

Key Laboratory for Research in Galaxies and Cosmology, Chinese Academy of Sciences, Hefei 230026, China
Department of Astronomy, University of Science and Technology of China, Hefei 230026, China; *yfyuan@ustc.edu.cn*

Received 2013 March 8; accepted 2013 July 5

Abstract We study the interaction between supermassive binary black holes in an elliptical orbit and their surrounding disk with a gap. The gap in the disk is a low density region formed due to the tidal effects of the less massive black hole. The binary we have investigated has a sub-parsec separation and is coplanar with the disk. We find that the maximum variation of the surface density in the gap reaches 50% during an orbital period. However, in other regions of the disk, the density variation is much less than 1%. Furthermore, we calculate the corresponding variation of spectral energy distribution within a period, but little variation is found. The reason for these results is that the viscosity timescale of the disk at the binary radius is much longer than the orbital period of the binary.

Key words: binaries: close — accretion disks — methods: numerical

1 INTRODUCTION

Supermassive binary black holes (SMBBHs) are believed to form during galaxy mergers, which frequently occur in the universe according to hierarchical models of galaxy formation. It is widely accepted that the merging of two supermassive black holes (SMBHs) goes through three stages (Begelman et al. 1980; Colpi & Dotti 2011). The standard picture is as follows. After the initial phase of merging of the galactic cores due to dynamical friction, the two SMBHs form a bound pair. The second phase in which the SMBBHs harden via 3-body scatterings off core stars is still uncertain. It is theoretically difficult to shrink the separation of SMBBHs by a factor of ~ 100 after its formation, which has a separation of ~ 1 pc (Merritt & Ekers 2002). This is known as the "final parsec problem." At the final phase, when SMBBHs reach a separation of ~ 0.01 pc, the two black holes will coalesce within a relatively short time interval through the emission of gravitational waves (GWs) (Sathyaprakash & Schutz 2009). Measuring the separation distribution between pairs of SMBHs helps to constrain the timescales of the different stages of the merging process for SMBHs and to estimate the number of GW sources that can be detected with the Laser Interferometer Space Antenna (LISA) in one year (Dotti et al. 2006).

* Supported by the National Natural Science Foundation of China.

Currently, there has been no direct detection of GWs, and the search for SMBBHs mainly focuses on the first and second phases of the merging process for SMBHs (Komossa 2006; Komossa et al. 2008; Colpi & Dotti 2011). Some SMBBHs, for instance, NGC 6240 (Komossa et al. 2003), COSMOS J100043.15+020637.2 (Comerford et al. 2009) and J0402+379 (Rodriguez et al. 2006), have been identified in a single galaxy via X-ray, optical and radio imaging spectroscopy. A few galaxies which contain double-peaked [O III] or Hβ lines with velocity offsets are suggested to contain pairs of active galactic nuclei (Zhou et al. 2004; Dotti et al. 2009; Wang et al. 2009; Shen & Loeb 2010; Liu et al. 2010). In addition, several other ways have been proposed to identify SMBBHs: X-shaped morphology of radio lobes (Merritt & Ekers 2002), double-double radio galaxies (Liu et al. 2003), orbital motion of the compact core which has a periodic flux variation (Sudou et al. 2003), periodic optical and radio outbursts (e.g., OJ 287) (Valtonen et al. 2008), and so on.

The eccentricity of SMBBHs in merging galaxies with a large amount of gas has been shown to be high (Roedig et al. 2011), which leads to periodic accretion flows onto the SMBH and then the periodic occurrence of peaked flares in light curves (Hayasaki et al. 2007). Hayasaki et al. (2012) carried out a smooth particle hydrodynamic simulation applied to a circumbinary disk with a central cavity and calculated the periodic mass accretion rate $\dot{M}$ onto the SMBHs. The corresponding periodic luminosity (luminosity $L = \eta \dot{M} c^2$) is believed to be the indicator of SMBBHs with sub-parsec separation. However, the mass accretion rate in their work is defined as the mass rate falling into a fixed "accretion" sphere without considering the detailed accretion physics. The radius of the fixed "accretion" sphere is chosen to be $0.1a$, where a is the semi-major axis of the binary orbit.

In this paper, the matter is accreted through a disk existing around the primary SMBH, rather than a defined "accretion" sphere. The matter across the gap flows onto the inner disk and is accreted into the primary SMBH by the effect of viscosity. This is a more realistic model that incorporates physical considerations.

The outline of this paper is as follows. In Section 2, we introduce the basic physics of the binary system, followed by a description of the simulation in Section 3. Finally, results and discussions are presented in Section 4.

2 PHYSICAL MODEL OF ACCRETION IN SMBBHS

2.1 Basic Equations Governing a Circumbinary Disk

It is assumed that a secondary SMBH exists in the accretion disk of the primary SMBH and its orbital plane is coplanar with the disk plane (Bogdanović et al. 2007; Dotti et al. 2010). The dynamics of this system are similar to those of a protoplanetary disk in the preliminary formation of a star. The latter has been widely discussed in the past decades (Goldreich & Tremaine 1980; Takeuchi et al. 1996; Espaillat et al. 2008). The hydrodynamic equations describing the evolution of a protoplanetary disk are described as follows (Kley 1999; Crida 2009):

$$\frac{\partial \Sigma}{\partial t} + \nabla \cdot (\Sigma \boldsymbol{u}) = 0\,, \tag{1}$$

$$\frac{\partial (\Sigma \upsilon)}{\partial t} + \nabla \cdot (\Sigma \upsilon \boldsymbol{u}) = \Sigma\, r(\omega + \Omega)^2 - \frac{\partial p}{\partial r} - \Sigma \frac{\partial \Phi}{\partial r} + f_r\,, \tag{2}$$

$$\frac{\partial [\Sigma r^2(\omega + \Omega)]}{\partial t} + \nabla \cdot [\Sigma r^2(\omega + \Omega)\boldsymbol{u}] = -\frac{\partial p}{\partial \varphi} - \Sigma \frac{\partial \Phi}{\partial \varphi} + f_\varphi\,. \tag{3}$$

These equations are expressed in cylindrical coordinates (r, φ, z), where r is the radial coordinate, φ is the azimuthal angle and z is the vertical axis. The reference frame rotates with angular velocity Ω. The rotation is around the z-axis, i.e. $\boldsymbol{\Omega} = (0, 0, \Omega)$. The disk is located in the $z = 0$ plane.

Equation (1) represents the conservation of mass. Σ denotes the surface density and $\boldsymbol{u}$ is the velocity vector of the fluid. Equations (2) and (3) represent the momentum equation in the r and φ directions respectively. The symbol $\upsilon = u_{\rm r}$ means radial velocity and $\omega = u_{\varphi}/r$ denotes the angular velocity of the flow, both of which are measured in the corotating frame. p is the vertically integrated (two-dimensional) pressure. The gravitational potential Φ is contributed by both the primary SMBH with mass $M_{\rm p}$ and the secondary BH with mass $M_{\rm s}$, which is given by

$$\Phi = -\frac{GM_{\rm p}}{|\boldsymbol{r}-\boldsymbol{r}_{\rm p}|}\left(1+\frac{M_{\rm s}|\boldsymbol{r}-\boldsymbol{r}_{\rm p}|}{M_{\rm p}|\boldsymbol{r}-\boldsymbol{r}_{\rm s}|}\right) = \Phi_0(1+\delta)\,,$$

where G is the gravitational constant and $\boldsymbol{r}_{\rm p}$ and $\boldsymbol{r}_{\rm s}$ are the position vectors of the primary and secondary BHs, respectively. Φ_0 is the gravitational potential induced by the primary SMBH and δ represents the potential perturbations induced by the secondary BH. If δ is small, Fourier decomposition of the time-periodic gravitational potential of the binary is applicable. The potential is given by a double series

$$\Phi(r,\theta,t) = \sum_{ml}\phi_{ml}(r){\rm e}^{[i(m\theta-l\Omega_B t)]}\,,$$

where l is the time-harmonic number, $m \geq 0$ is the azimuthal number, $\phi_{ml}(r)$ is the radially variable potential component,

$$\phi_{ml} = \frac{1}{2\pi^2}\int_0^{2\pi}\int_0^{2\pi}\Phi\cos(m\theta - l\Omega_B t)d\theta d(\Omega_B t)\,,$$

and $\Omega_B = (GM/a^3)^{1/2}$ is the mean motion of the binary, with M and a denoting the total mass and semimajor axis of the binary, respectively (Artymowicz & Lubow 1994). Two terms in Equations (2)–(3), $\frac{\partial\Phi}{\partial r}$ and $\frac{\partial\Phi}{\partial\varphi}$, act as tidal effects on the disk. f_r and f_φ represent the viscous force per unit area acting in the radial and azimuthal directions respectively. The explicit forms of f_r and f_φ are given by Kley (1999).

2.2 Resonance

Artymowicz & Lubow (1994) have analytically discussed the gravitational interaction of an eccentric binary star system with circumbinary gaseous disks. The interaction between the circular binary and the circumbinary disk can occur via an $(m,l)=(1,1)$ resonance (see Sect. 2.1 for the meaning of m,l) and higher noneccentric resonances like $(m,l)=(2,2)$, while the eccentric binary will induce resonances like $(m,l)=(2,1),(3,1),(4,1)$ or higher harmonics. The resonance will lead to tidal torque. When the total tidal torque at the edge of the disk is larger than the viscous torque, a gap opens in the disk (Lin & Papaloizou 1986). The condition for opening a gap in the $(1,1)$ circular resonance is given by

$$\alpha^{1/2}\left(\frac{H}{r}\right) \leq 0.24q(1-q)(1-2q)\,. \tag{4}$$

Here, q is the mass ratio between the SMBBHs. The circumbinary disk around the SMBBHs can be described an by α prescription (Shakura & Sunyaev 1973). r is the radius to the center of mass and H is the corresponding scale height of the disk at radius r.

For an eccentric binary, the $(m,l)=(2,1)$ and $(3,1)$ resonances become more important. The condition for opening a gap in the $(2,1)$ and $(3,1)$ resonances is given by

$$\alpha^{1/2}\left(\frac{H}{r}\right) \leq 1.76eq(1-q) \tag{5}$$

and

$$\alpha^{1/2}\left(\frac{H}{r}\right) \leq 1.42e^2q(1-q)(1-2q) \tag{6}$$

respectively. Here e is the eccentricity of the binary. If the values of α, $\frac{H}{r}$ and q are taken to be 0.05, 0.01 and 0.01, the minimum eccentricity to open the $(2,1)$ and $(3,1)$ resonance gaps is about 0.127 and 0.397, respectively.

2.3 Spectral Energy Distribution of the Disk

The disk is assumed to be in local thermal equilibrium, that is, the heating and cooling are locally balanced at each point of the disk, $Q_+ = Q_-$. The viscous heating term reads $Q_+ = 9\Sigma\nu\Omega^2/4$, where ν is the kinetic viscosity. The cooling term is given by the thermal emission, $Q_- = 2\sigma_R T_{\rm eff}^4$, where σ_R is the Stefan-Boltzmann constant and $T_{\rm eff}$ is the effective temperature of the disk. So, the effective temperature of each element in the disk is given by the equation

$$T_{\rm eff}(r,\varphi)^4 = \frac{9}{8}\frac{\nu}{\sigma}\Sigma(r,\varphi)\frac{GM}{r^3}. \tag{7}$$

The spectral energy distribution (SED) from a thermally emitting disk with the temperature being a function of radius can be written as

$$F_\lambda = \int_0^{2\pi}\int_{R_{\rm in}}^{R_{\rm out}} B_\lambda[T_{\rm eff}(r',\varphi')]g(r')r'dr'd\varphi', \tag{8}$$

where $B_\lambda(T_{\rm eff})$ is the Planck function and $g(r')$ is a function that describes the emissivity as a function of radius. We assume that $g(r') = 1$ where the disk material is present and $g(r') = 0$ elsewhere.

3 PHYSICAL MODEL AND PARAMETERS

We carry out a simulation using the FARGO-ADSG code (Baruteau & Masset 2008) in a two dimensional (R,ϕ) fixed polar grid. FARGO-ADSG is an extended version of FARGO (Masset 2000). In the FARGO-ADSG code, additional orbital advection, which removes the average azimuthal velocity, has been applied so that the truncation error is reduced and the timestep allowed by the Courant-Friedrichs-Lewy condition is significantly increased. The code was initially used to simulate the tidal planet-disk interactions. We adopt it because of the similarity between the planet-disk and the SMBBH-disk. The key parameters in the model are listed as follows:

Binary parameters— The mass of the primary and secondary black hole is taken to be $M_1 = 10^8 M_\odot$ and $M_2 = qM_1 = 4\times10^6 M_\odot$, respectively. This is common in galaxy-dwarf galaxy minor mergers whose mass ratio q ranges from 0.001 to 0.1. Despite the small mass ratio, recent numerical simulations have shown that local processes can lead these binaries to be sufficiently close (Bellovary et al. 2010). The initial semi-major axis a_0 and eccentricity e_0 of the binary are taken to be $10^3 r_{\rm g}(\approx 10^{-2}\ {\rm pc})$ and 0.5, respectively.

Disk parameters— Before its evolution, the disk is axisymmetric and rotates at Keplerian angular frequency $\Omega(r)$. The disk extends from $r = 10\,r_{\rm g}$ to $r = 4\times10^3\,r_{\rm g}$ in our simulation. The mesh is 256×156 in the polar coordinates (r,θ). The initial gas density of the disk is about $6.6\times10^5(r/a_0)^{-1/2}\ {\rm g\,cm^{-2}}$, which means that the initial disk mass is about $0.1M_1$. The aspect ratio $h = H/r$ is assumed to be 0.02 and remains constant throughout the simulation. In addition, the disk is modeled with a constant kinematic viscosity $\nu = 2\times10^{15}\ {\rm m^2\,s^{-1}}$, which corresponds to an alpha viscosity $\alpha \approx 0.05$ at 0.01 pc. The criteria for opening a gap are satisfied in our model.

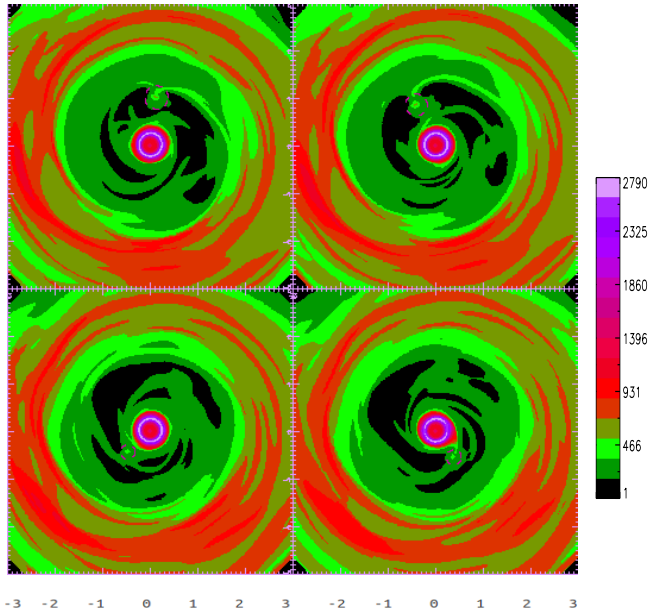

Fig. 1 Two-dimensional distributions of mass density at different orbital phases of the SMBBHs. *Top left* panel shows the result at the apocenter phase. *Bottom right* panel shows the result at the pericenter phase. *Top right* and *Bottom left* panels show two middle phases between the apocenter and pericenter phase, respectively. The dashed circles in dark pink show the Roche lobes of the secondary BH. The primary black hole is located at the center, and the coordinates are in units of $1000\,R_{\rm g}$ of the primary black hole. The density levels of each panel can be seen in the color bar on the right side. The black regions represent the minimum value of the surface density which is about 9.46×10^3 g cm^{-2}. The light purple regions represent the maximum value which is 2790 times the value of those in black. The other colors show the relative value of the surface density.

The inner boundary condition in the code is chosen to be open such that material can flow outside of the mesh, on its way to the central object. This results in a decrease of disk mass with time. The outer boundary condition which is not independent of the inner boundary condition cannot be selected in the code.

4 RESULTS AND DISCUSSION

In this work, the simulation runs until a stable gap is opened in the circumbinary disk of the SMBBHs. Our results are shown in Figures 1–3.

In Figure 1, we illustrate the two-dimensional surface density distribution of the disk when the binary has a stable eccentricity ($e = 0.3$). A gap is opened in the disk. The secondary SMBH causes the gas to flow across the gap when it moves from the apocenter to the pericenter. Furthermore, a high density ring exists in the inner disk, which can be attributed to the accumulation of matter.

In order to clearly show the variation of the surface density, the one-dimensional distribution of the surface density in one orbit is shown in Figure 2. The surface density varies significantly in the region around the gap (about $400\,R_{\rm g} \sim 1600\,R_{\rm g}$). The variation reaches 50% at $800\,R_{\rm g}$. However, the total amount of gas crossing the gap is still too low to change the surface density of the inner disk (less than 1% below $400\,R_{\rm g}$).

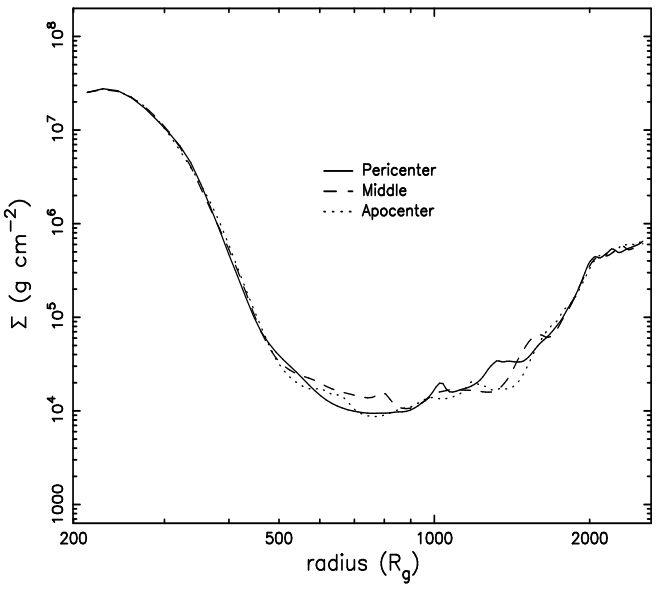

Fig. 2 One-dimensional distribution of the surface density within the radii between $220\,R_{\rm g}$ and $2600\,R_{\rm g}$.

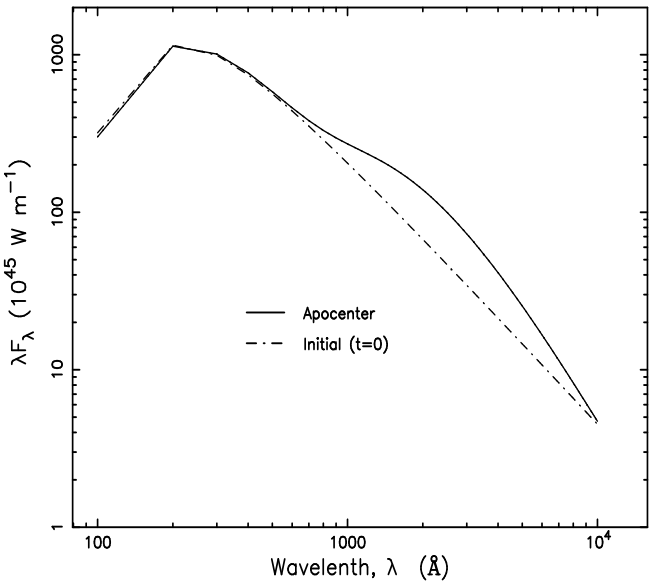

Fig. 3 SED of the radiation from the accreting flow in the system of SMBBHs. After a stable gap opens, the solid line represents the SED at the apocenter. The curves representing SEDs at other orbital phases (middle and pericenter) vary little compared with that at the apocenter and it is difficult to distinguish the curves at different orbital phases; hence they are not plotted in this figure. For comparison, the initial SED is shown by the dot-dashed line. At the initial moment, there is no gap in the disk.

It is meaningful to discuss the potential observational phenomena related to this process. Based on Equations (7) and (8), the emission fluxes at the various wavelengths are shown in Figure 3. There is little variation of the SED among the different orbital phases of the binary.

In this work we simulate the interaction between eccentric SMBBHs and their circumbinary disk. The surface density of the disk evolves under the action of binary torques in one orbital period. The orbital period is ~ 10 yr in our model. For comparison, we estimate the timescale of viscosity (therefore the accretion timescale) near the outer edge of the inner disk (about $400\,R_{\rm g}$). The timescale of viscosity is $t_{\rm visc} \sim R^2/\nu \sim 2.28 \times 10^5$ yr with our model parameters. It is obvious that the accretion timescale is much longer than the orbital period. Therefore, the gas across the gap only accumulates at the outer boundary of the inner disk. It is impossible for the accumulated gas to be accreted into the central SMBH in one orbital period. Consequently, the surface density of the inner disk does not significantly vary, as shown in Figure 2. The effective temperature in the disk is $T_{\rm eff} \propto \Sigma^{1/4}/r^{3/4}$, so the effective temperature of the inner disk, which has a larger surface density and smaller radius, is higher than that of the other regions. The emission from the inner disk, which shows little variation, dominates the thermal radiation of the disk. Therefore, the SED of the disk changes little, as shown in Figure 3.

It is natural to reduce the timescale of viscosity by increasing the value of the kinetic viscosity ν. However, as we argue below, this will negate the criteria needed for opening a gap. Equation (5) must be satisfied to open a gap in the disk if we take a (2:1) resonance gap as an example, which consequently results in a constraint on α. The kinetic viscosity is $\nu = \alpha h^2 a^2 \Omega_k$, and with the help of Equation (5), we get $\nu \leq 3e^2q^2(1-q)^2a^2\Omega_k$. Applying the typical parameters in our work ($e = 0.3, q = 0.04, a = 0.01$ pc, $\Omega_k = \sqrt{GM_{\rm p}/a^3} = 2.21 \times 10^{-8}$ rad s^{-1}), the kinetic viscosity at the binary radius satisfies $\nu \leq 8.55 \times 10^{17}$ m^2 s^{-1}. Therefore, the typical viscosity timescale at the orbital radius ($t_{\rm visc} \sim R^2/\nu \sim 3000$ yr) is at least 300 times longer than that of the binary period (~ 10 yr).

Recently, Bon et al. (2012) have shown that an SMBBH exists in the core of Seyfert galaxy NGC 4151. The periodic variations in the light curves and the radial velocity curves of NGC 4151 can be accounted for by an eccentric ($e = 0.42$), sub-parsec Keplerian orbit with a 15.9 yr period. The periodic variations in the observed shape of the H_α line and flux are well explained in the model with a shock that is generated by the supersonic motion of the SMBBHs through the surrounding medium, rather than the periodic disk accretion. We have argued that the periodic accretion of an eccentric binary with sub-parsec separation does not cause obvious variation in the SED. This is consistent with the result of Bon et al. (2012). As we adopt the α prescription of the disk in this work, it needs to be checked whether this prescription is still valid for a close SMBBH system. We hope that future observations of SMBBH candidates at sub-parsec separation will provide more information to constrain the properties of their accretion disks.

In this paper, the effect of GWs is neglected. We discuss the reason why below. The timescale of the orbital decay of the SMBBHs through GWs emission (Peters 1964) is

$$t_{\rm GW} \simeq 10^4 \frac{(1+q)^2}{q} \left(\frac{10^8 M_\odot}{M_{\rm total}}\right)^3 \left(\frac{a}{2\times 10^{-3}\ {\rm pc}}\right)^4 \frac{1}{f(e)}\ {\rm yr}.$$

Here, $f(e) = (1 + \frac{73e^2}{24} + \frac{37e^4}{96})(1-e^2)^{-7/2}$, where e is the eccentricity of the binary system. $t_{\rm GW}$ is about 8.8×10^7 yr in our model and is much longer than the viscous timescale ($t_{\rm visc} \simeq 10^6$ yr) at the orbital radius. Therefore it is reasonable to neglect the effect of GWs because the effect of viscosity is dominant.

The disk is modeled as a two-dimensional (r, φ) system, by using the vertically averaged quantities. Two main arguments lie behind this choice. First, on a physical basis, the Hill radius of a massive object is large or comparable to the disk semi-thickness. Second, a less massive secondary SMBH has a weak impact on the disk, requiring a higher resolution to properly compute and model

its effects. In the 2D simulation, it is easier to increase the resolution of the numerical simulation than in the 3D one. D'Angelo et al. (2003) showed that two-dimensional simulations still yield reliable results when the mass ratio $q \geq 10^{-4}$. When the mass ratio $q < 10^{-4}$, three-dimensional simulations are needed. The mass ratio is about 0.04 ($q = 0.04$) in our work, so the result might still be reliable.

Acknowledgements We would like to thank Prof. J. X. Wang for helpful discussions. This work is partially supported by the National Basic Research Program of China (973 Program, Grant Nos. 2009CB824800 and 2012CB821800), the National Natural Science Foundation of China (Grant Nos. 11073020, 11133005 and 11233003), and the Fundamental Research Funds for the Central Universities (WK2030220004).

References

Artymowicz, P., & Lubow, S. H. 1994, ApJ, 421, 651
Baruteau, C., & Masset, F. 2008, ApJ, 678, 483
Begelman, M. C., Blandford, R. D., & Rees, M. J. 1980, Nature, 287, 307
Bellovary, J. M., Governato, F., Quinn, T. R., et al. 2010, ApJ, 721, L148
Bogdanović, T., Reynolds, C. S., & Miller, M. C. 2007, ApJ, 661, L147
Bon, E., Jovanović, P., Marziani, P., et al. 2012, ApJ, 759, 118
Colpi, M., & Dotti, M. 2011, Advanced Science Letters, 4, 181
Comerford, J. M., Griffith, R. L., Gerke, B. F., et al. 2009, ApJ, 702, L82
Crida, A. 2009, ApJ, 698, 606
D'Angelo, G., Kley, W., & Henning, T. 2003, ApJ, 586, 540
Dotti, M., Colpi, M., & Haardt, F. 2006, MNRAS, 367, 103
Dotti, M., Montuori, C., Decarli, R., et al. 2009, MNRAS, 398, L73
Dotti, M., Volonteri, M., Perego, A., et al. 2010, MNRAS, 402, 682
Espaillat, C., Calvet, N., Luhman, K. L., Muzerolle, J., & D'Alessio, P. 2008, ApJ, 682, L125
Goldreich, P., & Tremaine, S. 1980, ApJ, 241, 425
Hayasaki, K., Mineshige, S., & Sudou, H. 2007, PASJ, 59, 427
Hayasaki, K., Saito, H., & Mineshige, S. 2012, arXiv:1211.5137
Kley, W. 1999, MNRAS, 303, 696
Komossa, S., Burwitz, V., Hasinger, G., et al. 2003, ApJ, 582, L15
Komossa, S. 2006, Mem. Soc. Astron. Italiana, 77, 733
Komossa, S., Zhou, H., & Lu, H. 2008, ApJ, 678, L81
Lin, D. N. C., & Papaloizou, J. 1986, ApJ, 309, 846
Liu, F. K., Wu, X.-B., & Cao, S. L. 2003, MNRAS, 340, 411
Liu, X., Shen, Y., Strauss, M. A., & Greene, J. E. 2010, ApJ, 708, 427
Masset, F. 2000, A&AS, 141, 165
Merritt, D., & Ekers, R. D. 2002, Science, 297, 1310
Peters, P. C. 1964, Physical Review, 136, 1224
Rodriguez, C., Taylor, G. B., Zavala, R. T., et al. 2006, ApJ, 646, 49
Roedig, C., Dotti, M., Sesana, A., Cuadra, J., & Colpi, M. 2011, MNRAS, 415, 3033
Sathyaprakash, B. S., & Schutz, B. F. 2009, Living Reviews in Relativity, 12, 2
Shakura, N. I., & Sunyaev, R. A. 1973, A&A, 24, 337
Shen, Y., & Loeb, A. 2010, ApJ, 725, 249
Sudou, H., Iguchi, S., Murata, Y., & Taniguchi, Y. 2003, Science, 300, 1263
Takeuchi, T., Miyama, S. M., & Lin, D. N. C. 1996, ApJ, 460, 832
Valtonen, M. J., Lehto, H. J., Nilsson, K., et al. 2008, Nature, 452, 851
Wang, J.-M., Chen, Y.-M., Hu, C., et al. 2009, ApJ, 705, L76
Zhou, H., Wang, T., Zhang, X., Dong, X., & Li, C. 2004, ApJ, 604, L33